

A Monte Carlo Study of the Second Virial Coefficient of Semiflexible Regular Three-Arm Star Polymers

By Daichi IDA and Takenao YOSHIZAKI*

A Monte Carlo (MC) study is made of the second virial coefficient A_2 along with the mean-square radius of gyration $\langle S^2 \rangle$ for regular three-arm star and linear freely rotating chains of bond angles θ ranging from 109° (typical flexible chain) to 175° (typical semiflexible or stiff chain) with the Lennard–Jones 6-12 potentials between beads corresponding to a good solvent system, in the range of the total number n of bonds from 30 to 900. On the basis of the MC values of A_2 so obtained, an examination is made of effects of chain stiffness on the ratio g_{A_2} of A_2 of the star chain to that of the linear one, both chains having the same n and θ . It is then found that g_{A_2} is rather insensitive to change in θ (chain stiffness) in contrast to the cases of the ratios g_S and g_η related to $\langle S^2 \rangle$ and the intrinsic viscosity $[\eta]$, respectively, which remarkably decrease with increasing θ .

KEY WORDS: Regular Three-Arm Star Polymer / Semiflexible Polymer / Second Virial Coefficient / Monte Carlo Simulation / Freely Rotating Chain /

In previous papers,^{1,2} we have examined effects of chain stiffness on the intrinsic viscosity $[\eta]$ of unperturbed regular three-arm star polymer chains by Monte Carlo (MC) simulations¹ or on the basis of the Kirkwood–Riseman theory.^{2–4} The ratio g_η of $[\eta]$ of an unperturbed regular three-arm star chain to that of an unperturbed linear one, both having the same molecular weight and chain stiffness, has been shown to become remarkably smaller than the value *ca.* 0.9 in the random-coil limit^{5,6} as the chains become stiffer, as in the case of the ratio g_S of the mean-square radius of gyration $\langle S^2 \rangle$ of the former chain to that of the latter.⁷ We note that g_S becomes 7/9 in the random-coil limit.⁸ Since $[\eta]$ and $\langle S^2 \rangle$ are measures of the average chain dimension, the above-mentioned results for g_η and g_S indicate that the average dimension of the unperturbed regular three-arm star chain becomes much smaller than that of the corresponding linear one as the chains become stiffer.

In good solvents (perturbed state), short-ranged repulsive interactions work between segments constituting the polymer chains, expanding the individual chains and yielding an effective volume V_E excluded to one chain by the presence of another. The volume V_E is another measure of the average chain dimension, although well-defined only in a good solvent system or in the perturbed state. The quantity V_E may be defined from the second virial coefficient A_2 as follows,⁴

$$A_2 = 4N_A V_E / M^2 \quad (1)$$

where N_A is the Avogadro constant and M is the molecular weight. It is then interesting to examine the effects of chain stiffness on the ratio g_{A_2} of A_2 of a regular three-arm star chain to that of the corresponding linear one. In this paper, we make an MC study of g_{A_2} as a necessary continuation of the previous papers.^{1,2}

An available theoretical value of g_{A_2} for the regular three-arm star chain is 0.968 in the random-coil limit obtained by Douglas and Freed⁹ on the basis of the polymer renormalization group (RG) theory, being nearly equal to unity. Then the main question we must answer in this paper is whether or not g_{A_2} becomes remarkably smaller than unity as the chains become stiffer, as in the cases of g_η and g_S .

MODELS AND METHODS

The MC models used in this study are the same as those used in the previous one¹ except for the value of a parameter of interactions between segments (beads).

The star chain model is the regular three-arm star freely rotating chain, each arm composed of m successive bonds of length unity, so that it is composed of $3m$ ($= n$) bonds, in total, and $3m + 1$ beads whose centers are located at $3m - 3$ junctions of two successive bonds on the arms, at the three terminal ends, and at the branch point (center) (see Figure 1 of ref 1). The angle between each pair of the bonds connected to the center is fixed to be 120° , so that those bonds are on the same plane. For convenience, the three arms are designated the first, second, and third ones and the beads on the i th arm ($i = 1, 2, 3$) are numbered $(i - 1)m + 1, (i - 1)m + 2, \dots, im$ from the center to the end, with the center bead numbered 0. The i th bond vector ($1 \leq i \leq 3m; i \neq m + 1, 2m + 1$) connects the centers of the $(i - 1)$ th and i th beads with its direction from the $(i - 1)$ th to i th bead, and the $(m + 1)$ th and $(2m + 1)$ th bond vectors are from the 0th to the $(m + 1)$ th and $(2m + 1)$ th beads, respectively. All the $3m - 3$ bond angles θ (not supplement) except for those around the center are fixed, so that the configuration of the entire chain may be specified by the set of $3m - 3$ rotation angles $\{\phi_{3m-3}\} = (\phi_1, \dots, \phi_{m-1}, \phi_{m+1}, \dots, \phi_{2m-1}, \phi_{2m+1}, \dots, \phi_{3m-1})$ apart from its position and orientation

Department of Polymer Chemistry, Kyoto University, Katsura, Kyoto 615-8510, Japan

*To whom correspondence should be addressed (E-mail: yoshizaki@molsci.polym.kyoto-u.ac.jp).

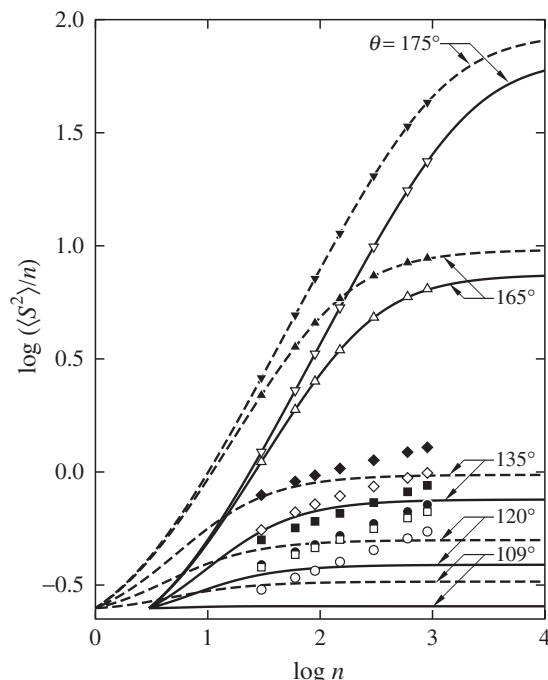


Figure 1. Double-logarithmic plots of $\langle S^2 \rangle/n$ against n at $T^* = 8.0$ (good solvent system). The open and closed symbols represent the MC values for the regular three-arm star and linear freely rotating chains, respectively, of $\theta = 109^\circ$ (\circ , \bullet), 120° (\square , \blacksquare), 135° (\diamond , \blacklozenge), 165° (\triangle , \blacktriangle), and 175° (∇ , \blacktriangledown). The solid and dashed curves represent the theoretical values for the ideal regular three-arm star and linear freely rotating chains, respectively, with the indicated values of θ .

in an external Cartesian coordinate system, where ϕ_i is the internal rotation angle around the i th bond vector.

The linear chain model, the counterpart of the above star one, is the freely rotating chain composed of n bonds of length unity and $n + 1$ beads, whose centers are located at the $n - 1$ junctions of two successive bonds and at the two terminal ends. We set n equal to $3m$. The beads are numbered $0, 1, 2, \dots, n$ from one end to the other, and the i th bond vector ($i = 1, 2, \dots, n$) connects the centers of the $(i - 1)$ th and i th beads with its direction from the $(i - 1)$ th to the i th bead. All the $n - 1$ bond angles are fixed at θ , so that the configuration of the linear chain may be specified by the set of $n - 2$ internal rotation angles $\{\phi_{n-2}\} = (\phi_2, \phi_3, \dots, \phi_{n-1})$ apart from its position and orientation in the external Cartesian coordinate system.

The total potential energy U of the regular three-arm star chain as a function of $\{\phi_{3m-3}\}$ may be given by

$$\begin{aligned}
 U(\{\phi_{3m-3}\}) = & \sum_{i=0}^1 \sum_{j=i+1}^2 \sum_{k,l=1}^m h(k+l-4) u(R_{(im+k)(jm+l)}) \\
 & + \sum_{i=0}^2 \sum_{j=1}^{m-4} \sum_{k=j+4}^m u(R_{(im+j)(im+k)}) \\
 & + \sum_{i=0}^2 \sum_{j=4}^m u(R_{0(im+j)})
 \end{aligned}
 \tag{2}$$

(regular three-arm star)

and that of the linear one as a function of $\{\phi_{n-2}\}$ by

$$U(\{\phi_{n-2}\}) = \sum_{i=0}^{n-4} \sum_{j=i+4}^n u(R_{ij}) \quad (\text{linear}) \tag{3}$$

where $h(x)$ is a unit step function such that $h(x) = 1$ for $x \geq 0$ and $h(x) = 0$ for $x < 0$ and R_{ij} is the distance between the centers of the i th and j th beads. We note that in eqs 2 and 3 the interactions between the third-neighbor beads along the chain have been neglected, since they seem to make the chain locally take the *cis* conformation to excess.

Similarly, the total intermolecular (excluded-volume) potential energy $U_{12}(1, 2)$ between two chains 1 and 2 as a function of all the coordinates of chains 1 and 2 may be given by

$$U_{12}(1, 2) = \sum_{i_1=0}^n \sum_{i_2=0}^n u(R_{i_1 i_2}) \tag{4}$$

where $R_{i_1 i_2}$ is the distance between the centers of the i_1 th bead of chain 1 and of the i_2 th one of chain 2. We note that we use the McMillan–Mayer symbolism^{4,10} to formulate A_2 , here and hereafter. Then the i th bead ($i = 0, 1, 2, \dots, n$) of chain α ($\alpha = 1, 2$) is labeled as i_α , and the symbol (α) ($\alpha = 1, 2$) denotes all the coordinates (external and internal) of chain α .

We adopt as the pair potential $u(R)$ (of mean force) the cutoff version of the Lennard–Jones (LJ) 6-12 potential given by

$$\begin{aligned}
 u(R) = & \infty & \text{for } 0 \leq R < c\sigma \\
 = & u^{\text{LJ}}(R) & \text{for } c\sigma \leq R < 3\sigma \\
 = & 0 & \text{for } 3\sigma \leq R
 \end{aligned} \tag{5}$$

where $u^{\text{LJ}}(R)$ is the LJ potential¹¹ given by

$$u^{\text{LJ}}(R) = 4\epsilon \left[\left(\frac{\sigma}{R} \right)^{12} - \left(\frac{\sigma}{R} \right)^6 \right] \tag{6}$$

with σ and ϵ the collision diameter and the depth of the potential well at the minimum of $u^{\text{LJ}}(R)$, respectively. We note that $u(R)$ given by eq 5 is the LJ potential cut off at the upper bound 3σ . The lower bound $c\sigma$ in eq 5 has been introduced for numerical convenience; the factor c is properly chosen so that the Boltzmann factor $e^{-u^{\text{LJ}}/k_B T}$ may be regarded as numerically vanishing compared to unity, where k_B is the Boltzmann constant and T is the absolute temperature. In practice, in double-precision computation, we put

$$c = [2/(1 + \sqrt{1 + 36T^*})]^{1/6} \tag{7}$$

so that $e^{-u^{\text{LJ}}/k_B T} \lesssim 2 \times 10^{-16}$ for $0 \leq R < c\sigma$, where T^* is the reduced temperature defined by $T^* = k_B T/\epsilon$. Further, we put $\sigma = 1$ for simplicity, as previously¹ done. We note that the value 3.72 of T^* corresponds to the Θ temperature and 8.0 to a good solvent system.^{12,13}

The mean-square radius of gyration $\langle S^2 \rangle$, *i.e.*, the ensemble average of the square radius of gyration S^2 may be evaluated from

$$\langle S^2 \rangle = N_s^{-1} \sum_{\{\phi_k\}} S^2(\{\phi_k\}) \tag{8}$$

where the sum is taken over N_s sample configurations $\{\phi_k\}$ with k being equal to $3m - 3$ for the star chain and $n - 2$ for the

linear one, $\{\phi_k\}$ generated in an MC run by an application of the pivot algorithm^{14,15} and the Metropolis method of importance sampling¹⁶ as done in the previous MC studies.^{1,12} For each sample configuration, S^2 as a function of $\{\phi_k\}$ may be calculated from

$$S^2 = \frac{1}{n+1} \sum_{i=0}^n |\mathbf{r}_i - \mathbf{r}_{c.m.}|^2 \quad (9)$$

with \mathbf{r}_i the vector position of the center of the i th bead and $\mathbf{r}_{c.m.}$ the vector position of the center of mass of the chain given by

$$\mathbf{r}_{c.m.} = \frac{1}{n+1} \sum_{i=0}^n \mathbf{r}_i \quad (10)$$

In every MC run, an initial configuration is generated by trial and error so that all the distances between the centers of beads are greater than or equal to c . (Note that $\sigma = 1$.) One configuration is sampled at every M_{nom} (nominal) pivot steps, so that $N_s \times M_{nom}$ pivot steps are required to obtain a set of N_s sample configurations. The number of M_{nom} has been chosen to be *ca.* $10n$ for the regular three-arm star chains and *ca.* $2n$ for the linear ones.

As for the second virial coefficient A_2 , it may be evaluated from

$$A_2 = \frac{2\pi N_A}{M^2} \int_0^\infty \left\{ 1 - \exp\left[-\frac{\bar{U}_{12}(r)}{k_B T}\right] \right\} r^2 dr \quad (11)$$

where $\bar{U}_{12}(r)$ is the averaged intermolecular potential as a function of the distance $r = |\mathbf{r}|$ between the centers of mass of chains 1 and 2 defined by

$$\bar{U}_{12}(r) = -k_B T \ln \left\langle \exp\left[-\frac{U_{12}(1,2)}{k_B T}\right] \right\rangle_r \quad (12)$$

In eq 12, $\langle \dots \rangle_r$ indicates the conditional equilibrium average taken over the configurations of the two chains with \mathbf{r} fixed by the use of the single-chain distribution function for each with the intramolecular excluded-volume potential for the star and linear chains given by eqs 2 and 3, respectively. In practice, the conditional average may be calculated by the use of a set of N_s sample configurations $\{\phi_k\}$ generated above, as follows. First, we randomly sample a pair of sample configurations (chains 1 and 2) from the set and calculate the intermolecular potential U_{12} from eq 4 at given r after randomizing the orientations of the two configurations in the external coordinate system. Numerical evaluation of U_{12} may be carried out following the procedure used in the previous study¹³ of A_2 with the use of the “zippering” method.^{17,18} Then the average on the right-hand side of eq 12 may be evaluated from

$$\left\langle \exp\left[-\frac{U_{12}(1,2)}{k_B T}\right] \right\rangle_r = N_p^{-1} \sum'_{(1,2)} \exp\left[-\frac{U_{12}(1,2)}{k_B T}\right] \quad (13)$$

where $\sum'_{(1,2)}$ indicates summation over N_p pairs of sample configurations (1,2) at given r . With the values of $\bar{U}_{12}(r)$ so evaluated for various values of r at given T^* , the quantity $A_2 M^2$ for given n may then be calculated from eq 11 by numerical integration with the use of the trapezoidal rule formula.

In the practical evaluation of $\langle S^2 \rangle$ and A_2 for the regular three-arm star and linear freely rotating chains at $T^* = 8.0$ (good solvent system), we have generated 10 sets of 10^5 ($= N_s$) sample configurations for $n = 30, 60, 90, 150$, and 300 , 5 sets of those for $n = 600$, and 2 sets of those for $n = 900$. In the evaluation of \bar{U}_{12} (and A_2), 10^6 or 10^7 ($= N_p$) sample pairs have been taken from each set. Then the total number of sample pairs is equal to the number N_p of sample pairs in each set multiplied by the number of sets.

All the numerical work has been done by the use of a personal computer with an Intel Core2 Duo E6600 CPU. A source program coded in C has been compiled by the GNU C compiler version 3.4.6 with real variables of double precision. For a generation of pseudorandom numbers, the subroutine package MT19937 supplied by Matsumoto and Nishimura¹⁹ has been used instead of the subroutine RAND included in the standard C library.

RESULTS AND DISCUSSION

Mean-Square Radius of Gyration

We have carried out MC runs to generate sample configurations for the regular three-arm star and linear freely rotating chains with n ($= 3m$) = 30, 60, 90, 150, 300, 600, and 900 and $\theta = 109^\circ, 120^\circ, 135^\circ, 165^\circ$, and 175° at $T^* = 8.0$ (good solvent system). The chain of $\theta = 109^\circ$ corresponds to a typical flexible chain, and the chain becomes stiffer with increasing θ from 109° to 175° .

The MC values of $\langle S^2 \rangle/n$ for the star and linear chains are given in the second and fourth columns, respectively, of Table I, the number in the parentheses attached to each value indicating its statistical error. The $\langle S^2 \rangle/n$ value and its error for each chain are the mean and the standard deviation, respectively, of independent MC results.

Figure 1 shows double-logarithmic plots of $\langle S^2 \rangle/n$ against n at $T^* = 8.0$ (good solvent system). The open and closed symbols represent the MC values for the star and linear chains, respectively, of $\theta = 109^\circ$ (\circ, \bullet), 120° (\square, \blacksquare), 135° (\diamond, \blacklozenge), 165° ($\triangle, \blacktriangle$), and 175° ($\nabla, \blacktriangledown$). The solid and dashed curves represent the theoretical values of $\langle S^2 \rangle/n$ for the ideal regular three-arm star and linear freely rotating chains, respectively, without interactions between beads, which have been calculated from

$$\begin{aligned} \langle S^2 \rangle = & \frac{7}{54} \frac{1 - \cos \theta}{1 + \cos \theta} n + \frac{1}{54} \frac{31 + 90 \cos \theta - 13 \cos^2 \theta}{(1 + \cos \theta)^2} \\ & + \frac{1}{18} \frac{19 + 49 \cos \theta + 71 \cos^2 \theta + 5 \cos^3 \theta}{(1 + \cos \theta)^3} \frac{1}{n+1} \\ & - \frac{2(1 + 2 \cos \theta)}{(1 + \cos \theta)^3} \frac{1 - (-\cos \theta)^{n/3+1}}{n+1} \\ & + \frac{1}{27} \frac{(1 - \cos \theta)(37 - 16 \cos \theta + \cos^2 \theta)}{(1 + \cos \theta)^3} \frac{1}{(n+1)^2} \\ & - \frac{2(2 + \cos^2 \theta)}{(1 + \cos \theta)^4} \frac{1 - (-\cos \theta)^{n/3+1}}{(n+1)^2} \end{aligned}$$

Table I. Values of $\langle S^2 \rangle/n$ and $A_2 M_b^2/N_A$ at $T^* = 8.0$ (good solvent system)

n	three-arm star		linear	
	$\langle S^2 \rangle/n$ (error%)	$A_2 M_b^2/N_A$ (error%)	$\langle S^2 \rangle/n$ (error%)	$A_2 M_b^2/N_A$ (error%)
$\theta = 109^\circ$				
30	0.302 ₀ (0.1)	0.251 ₅ (0.1)	0.389 ₃ (0.1)	0.261 ₅ (0.2)
60	0.340 ₇ (0.1)	0.203 ₄ (0.1)	0.443 ₃ (0.1)	0.213 ₄ (0.2)
90	0.366 ₁ (0.1)	0.181 ₈ (0.1)	0.477 ₃ (0.1)	0.191 ₅ (0.1)
150	0.400 ₄ (0.1)	0.159 ₀ (0.1)	0.523 ₄ (0.1)	0.168 ₄ (0.1)
300	0.451 ₅ (0.1)	0.133 ₆ (0.1)	0.591 ₅ (0.1)	0.142 ₁ (0.1)
600	0.508 ₈ (0.1)	0.113 ₁ (0.1)	0.667 ₇ (0.1)	0.120 ₃ (0.2)
900	0.545 ₈ (0.1)	0.102 ₅ (0.0)	0.716 ₉ (0.1)	0.109 ₅ (0.1)
$\theta = 120^\circ$				
30	0.379 ₄ (0.1)	0.285 ₉ (0.1)	0.500 ₉ (0.1)	0.301 ₁ (0.2)
60	0.431 ₁ (0.1)	0.241 ₄ (0.1)	0.565 ₉ (0.1)	0.252 ₉ (0.2)
90	0.462 ₂ (0.1)	0.218 ₉ (0.1)	0.604 ₈ (0.1)	0.229 ₈ (0.1)
150	0.502 ₆ (0.1)	0.194 ₂ (0.1)	0.656 ₀ (0.1)	0.205 ₀ (0.1)
300	0.561 ₃ (0.1)	0.165 ₉ (0.2)	0.732 ₆ (0.1)	0.175 ₇ (0.1)
600	0.626 ₀ (0.1)	0.141 ₈ (0.1)	0.817 ₃ (0.1)	0.150 ₅ (0.2)
900	0.667 ₅ (0.0)	0.129 ₃ (0.1)	0.872 ₃ (0.0)	0.137 ₅ (0.0)
$\theta = 135^\circ$				
30	0.553 ₇ (0.1)	0.327 ₄ (0.2)	0.790 ₁ (0.1)	0.336 ₂ (0.2)
60	0.663 ₅ (0.1)	0.287 ₃ (0.3)	0.907 ₉ (0.2)	0.297 ₃ (0.1)
90	0.720 ₁ (0.1)	0.268 ₄ (0.1)	0.966 ₆ (0.2)	0.278 ₈ (0.2)
150	0.782 ₉ (0.1)	0.246 ₃ (0.2)	1.03 ₆ (0.1)	0.256 ₉ (0.2)
300	0.862 ₆ (0.1)	0.219 ₀ (0.1)	1.12 ₇ (0.1)	0.229 ₄ (0.1)
600	0.941 ₄ (0.1)	0.193 ₅ (0.1)	1.22 ₄ (0.1)	0.203 ₁ (0.1)
900	0.990 ₄ (0.0)	0.179 ₇ (0.0)	1.28 ₅ (0.1)	0.188 ₇ (0.0)
$\theta = 165^\circ$				
30	1.10 ₉ (0.0)	0.355 ₆ (0.4)	2.18 ₅ (0.0)	0.352 ₄ (0.4)
60	1.88 ₆ (0.0)	0.330 ₇ (0.3)	3.57 ₁ (0.0)	0.331 ₄ (0.4)
90	2.51 ₆ (0.0)	0.323 ₃ (0.4)	4.56 ₁ (0.1)	0.323 ₆ (0.6)
150	3.46 ₁ (0.0)	0.316 ₁ (0.3)	5.85 ₁ (0.1)	0.317 ₇ (0.2)
300	4.82 ₃ (0.1)	0.310 ₀ (0.3)	7.37 ₈ (0.1)	0.311 ₆ (0.3)
600	5.95 ₁ (0.1)	0.304 ₄ (0.1)	8.42 ₈ (0.1)	0.307 ₅ (0.1)
900	6.44 ₄ (0.1)	0.303 ₀ (0.1)	8.82 ₉ (0.0)	0.305 ₂ (0.3)
$\theta = 175^\circ$				
30	1.22 ₆ (0.0)	0.354 ₃ (0.3)	2.60 ₅ (0.0)	0.343 ₈ (0.6)
60	2.29 ₂ (0.0)	0.327 ₉ (0.4)	4.93 ₆ (0.0)	0.320 ₁ (0.8)
90	3.33 ₀ (0.0)	0.319 ₁ (0.5)	7.16 ₄ (0.0)	0.311 ₈ (0.5)
150	5.32 ₈ (0.0)	0.310 ₉ (0.3)	11.3 ₄ (0.0)	0.307 ₃ (0.8)
300	9.90 ₀ (0.0)	0.304 ₁ (0.5)	20.3 ₄ (0.0)	0.302 ₉ (0.5)
600	17.5 ₃ (0.1)	0.301 ₈ (0.3)	33.7 ₄ (0.1)	0.299 ₉ (0.9)
900	23.5 ₉ (0.1)	0.299 ₇ (0.5)	43.0 ₃ (0.1)	0.297 ₀ (0.6)

$$+ \frac{3}{(1 + \cos \theta)^4} \frac{[1 - (-\cos \theta)^{n/3+1}]^2}{(n+1)^2} \quad (\text{regular three-arm star}) \quad (14)$$

and

$$\langle S^2 \rangle = \frac{1}{6} \frac{1 - \cos \theta}{1 + \cos \theta} n + \frac{1}{6} \frac{1 + 6 \cos \theta - \cos^2 \theta}{(1 + \cos \theta)^2} + \frac{1}{6} \frac{-1 - 7 \cos \theta + 7 \cos^2 \theta + \cos^3 \theta}{(1 + \cos \theta)^3} \frac{1}{n+1} - \frac{2 \cos^2 \theta}{(1 + \cos \theta)^4} \frac{1 - (-\cos \theta)^{n+1}}{(n+1)^2} \quad (\text{linear}) \quad (15)$$

respectively, with the indicated values of θ . We note that eq 14 is a special case of the theoretical expression obtained by Guenza *et al.*²⁰ for the regular f -arm star freely rotating chain.

In the cases of $\theta = 109^\circ$, 120° and 135° , the MC values for both the star and linear chains deviate upward from the corresponding ideal-chain ones because of the intramolecular excluded-volume effect and also of the effect of the interactions between beads on the unperturbed chain dimension through the short-range interference.^{12,21,22} In the cases of $\theta = 165^\circ$ and 175° , on the other hand, the MC values for both the star and linear chains are almost identical with the corresponding ideal-chain values, because the effects of the intramolecular interactions between beads become negligibly small for a

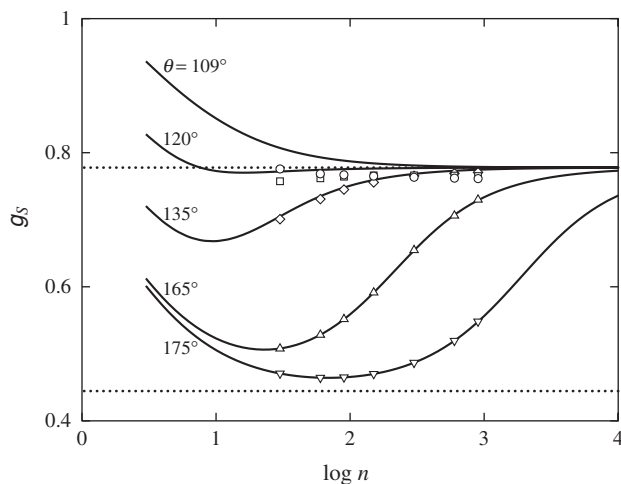


Figure 2. Plots of g_S against $\log n$ at $T^* = 8.0$ (good solvent system) for the freely rotating chains of $\theta = 109^\circ$ (\circ), 120° (\square), 135° (\diamond), 165° (\triangle), and 175° (∇). The solid curves represent the theoretical values for the ideal freely rotating chains with the indicated values of θ . The upper and lower dotted horizontal lines represent the asymptotic values $7/9$ in the ideal random-coil limit and $4/9$ in the rigid-rod limit, respectively.

typical stiff chain if its total contour length is not very long. We note that the ring-closure or intramolecular-contact probability approaches zero in the rigid-rod limit and therefore the intramolecular excluded-volume effect vanishes in the limit.

Figure 2 shows plots of g_S against $\log n$ at $T^* = 8.0$ (good solvent system), where g_S is the ratio of $\langle S^2 \rangle$ of the regular three-arm star chain to that of the corresponding linear one. The symbols represent the MC values of g_S calculated from the values of $\langle S^2 \rangle/n$ given in the second and fourth columns in Table I for $\theta = 109^\circ$ (\circ), 120° (\square), 135° (\diamond), 165° (\triangle), and 175° (∇). The solid curves represent the theoretical values for the ideal chains calculated from eqs 14 and 15. The upper and lower dotted horizontal lines represent the asymptotic values $7/9$ in the ideal (unperturbed) random-coil limit⁸ and $4/9$ in the rigid-rod limit,⁷ respectively.

In the case of $\theta = 109^\circ$ (typical flexible chain), the MC value 0.76 of g_S for $n = 900$ is somewhat (*ca.* 2%) smaller than the value $7/9$ ($= 0.778$) in the ideal random-coil limit. The available experimental values of g_S for regular f -arm star polystyrenes (PS) in good solvents obtained by Khasat *et al.*²³ for $f = 3$ and by Okumoto *et al.*^{24,25} for $f = 4$ and 6 are 0.79 , 0.61 , and 0.45 , respectively, and are in good agreement with the respective ideal random-coil limiting values $7/9$ ($= 0.778$), $5/8$ ($= 0.625$), and $4/9$ ($= 0.444$), which have been calculated from $g_S = (3f - 2)/f^2$.⁸ The available theoretical values of g_S obtained by Douglas and Freed⁹ on the bases of the polymer RG theory for the regular three-, four-, and six-arm stars in the perturbed random-coil limit are 0.778 , 0.631 , and 0.453 , respectively, and are consistent with the experimental ones. Then the present MC result for long flexible chains is consistent with the above-mentioned experimental and theoretical results.

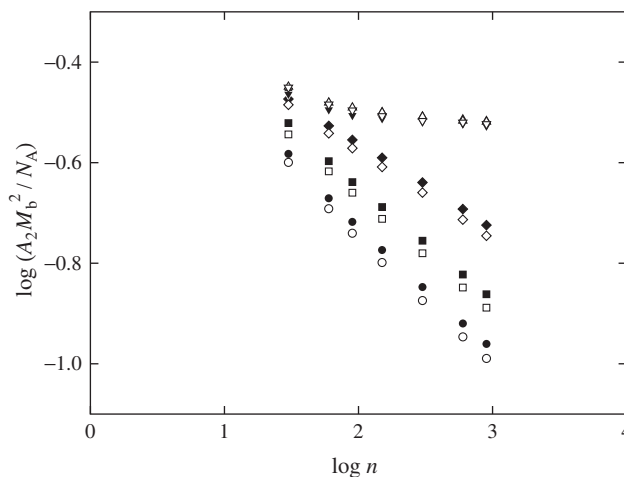


Figure 3. Double-logarithmic plots of $A_2 M_b^2 / N_A$ against n at $T^* = 8.0$ (good solvent system). All the symbols have the same meaning as those in Figure 1.

As a natural consequence of the results shown in Figure 1, the MC value of g_S becomes almost identical with the ideal chain value as the chain becomes stiffer. The ratio g_S , on the whole, remarkably depends on the chain stiffness but scarcely on the intramolecular excluded volume.

Second Virial Coefficient

We have numerically evaluated $A_2 M_b^2 / N_A$ from eqs 11–13 on the basis of the sets of sample configurations generated in the above-mentioned MC evaluation of $\langle S^2 \rangle$. The MC values of $A_2 M_b^2 / N_A$ with $M_b = M/n$ so obtained for the star and linear chains are given in the third and fifth columns, respectively, of Table I, the number in the parentheses attached to each value indicating its statistical error. The $A_2 M_b^2 / N_A$ value and its error for each chain are the mean and the standard deviation, respectively, of independent MC results.

Figure 3 shows double-logarithmic plots of $A_2 M_b^2 / N_A$ against n at $T^* = 8.0$ (good solvent system), where all the open and closed symbols have the same meaning as those in Figure 1. In the case of $\theta = 109^\circ$ (typical flexible chain), the value for the regular three-arm star is somewhat (6% at most) smaller than the corresponding value for the linear chain. For both the star and linear chains, A_2 decreases with increasing n and the slopes of the plots become almost identical with the asymptotic value -0.2 for very large n . The difference in the value of A_2 between the two chains becomes small and the slopes become gentle, as θ (chain stiffness) is increased. In the case of $\theta = 175^\circ$ (typical semiflexible or stiff chain), A_2 becomes almost independent of n for $n \geq 100$, as in the case of the rigid rod.

It is interesting to note that the value of A_2 for the chain of $\theta = 175^\circ$ is smaller than that of $\theta = 165^\circ$ over the whole range of n examined. It may be regarded as arising from the fact that two chains with the LJ potential (having the attractive interaction), which are close to each other, prefer to be parallel rather than perpendicular to each other when their stiffness becomes large and their A_2 may therefore be suppressed,²⁶ as

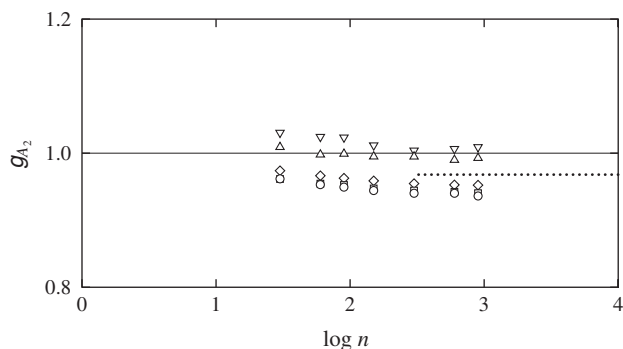


Figure 4. Plots of g_{A_2} against $\log n$ at $T^* = 8.0$ (good solvent system). All the symbols have the same meaning as those in Figure 2. The dotted horizontal line segment represents the RG theory value⁹ 0.968.

discussed by Schoot and Odijk²⁷ in the case of long rigid rods with a van der Waals-type potential.

Figure 4 shows plots of g_{A_2} against $\log n$ at $T^* = 8.0$ (good solvent system). The symbols, which have the same meaning as those in Figure 2, represent the MC values of g_{A_2} calculated from the values of $A_2 M_b^2 / N_A$ given in the third and fifth columns in Table I. We note that from the defining eq 1 for the effective intermolecular excluded volume V_E , g_{A_2} may be written in terms of V_E as follows,

$$g_{A_2} = \frac{A_2(\text{star})}{A_2(\text{linear})} = \frac{V_E(\text{star})}{V_E(\text{linear})} \quad (16)$$

In the case of $\theta = 109^\circ$ (typical flexible chain), g_{A_2} slightly decreases with increasing n and then seems to approach a constant independent of n . The asymptotic value of g_{A_2} in the limit of $n \rightarrow \infty$ may be estimated to be 0.94 which is the mean of the three MC values 0.94₀, 0.94₀, and 0.93₆ for $n = 300$, 600, and 900, respectively. The g_{A_2} value so obtained is rather in good agreement with the RG theory value⁹ 0.968 represented by the dotted horizontal line segment in Figure 4. In this connection, we refer to literature experimental and theoretical values of g_{A_2} for regular stars. The former values are 0.89 and 0.79 for the regular four- and six-arm star PSs,^{24,25} respectively, and they are rather in good agreement with the corresponding RG theory values⁹ 0.923 and 0.808. Strictly speaking, the RG theory values are somewhat (*ca.* 3%) larger than the corresponding experimental and present MC values.

It is more important to see in Figure 4 that g_{A_2} slightly increases with increasing θ (chain stiffness) in the range of θ from 109° to 165° and it becomes almost identical with unity for $\theta = 165^\circ$ and 175° in the range of $n \gtrsim 100$. We note that g_{A_2} in the cases of $\theta = 165^\circ$ and 175° approaches, of course, the above-mentioned asymptotic value in the limit of $n \rightarrow \infty$. In contrast to the cases of g_S and g_η , g_{A_2} is rather insensitive to change in θ (chain stiffness). Such characteristic behavior of g_{A_2} may be regarded as arising from the fact that in terms of the (classical) perturbation theory,⁴ effects of the multiple intermolecular contact become negligibly small, if any, in the rigid-rod limit. The decreases in A_2 of the star and linear chains

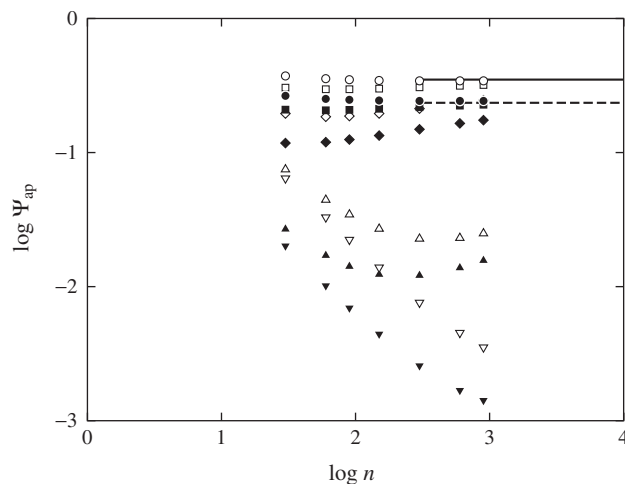


Figure 5. Double-logarithmic plots of Ψ_{ap} against n at $T^* = 8.0$ (good solvent system). All the symbols have the same meaning as those in Figure 1. The solid horizontal line segment represents the asymptotic value 0.35 in the random-coil limit obtained by Ohno *et al.*³¹ for the self-avoiding regular three-arm star chain on the simple cubic lattice and the dashed one the corresponding value 0.235 obtained by Barrett³² for the self-avoiding linear chain on the same lattice.

due to the attractive interaction in the LJ potential may be considered to cancel out with each other in g_{A_2} .

Finally, we consider the *apparent* interpenetration function Ψ_{ap} defined by²⁸

$$A_2 = 4\pi^{3/2} N_A \frac{\langle S^2 \rangle^{3/2}}{M^2} \Psi_{\text{ap}} \quad (17)$$

from the *whole* A_2 including effects of chain ends.^{29,30} Figure 5 shows double-logarithmic plots of Ψ_{ap} against n at $T^* = 8.0$ (good solvent system). The open and closed symbols, which have the same meaning as those in Figures 1 and 3, represent the MC values for the star and linear chains, respectively, calculated from eq 17 with the values of $\langle S^2 \rangle / n$ and $A_2 M_b^2 / N_A$ given in Table I.

In the case of $\theta = 109^\circ$ (typical flexible chain), Ψ_{ap} for both the star and linear chains slightly decreases with increasing n and then seems to approach the asymptotic values 0.34 and 0.24, respectively, which are the means of the three Ψ_{ap} values for $n = 300$, 600, and 900, although Ψ_{ap} is appreciably larger for the star chain than for the linear one. The two asymptotic values are in good agreement with the literature MC values 0.35 for the star chain and 0.235 for the linear one obtained by Ohno *et al.*³¹ and Barrett,³² respectively, by the use of self-avoiding chains on the simple cubic lattice. In Figure 5, the two literature values for the star and linear chains are represented by the solid and dashed horizontal line segments, respectively. We note that the RG theory values⁹ 0.384 and 0.269 of Ψ_{ap} for the perturbed flexible regular three-arm star and linear chains, respectively, are somewhat (*ca.* 10%) larger than the above-mentioned present and literature MC values. As θ (chain stiffness) is increased from 109° to 175° , Ψ_{ap} decreases monotonically.

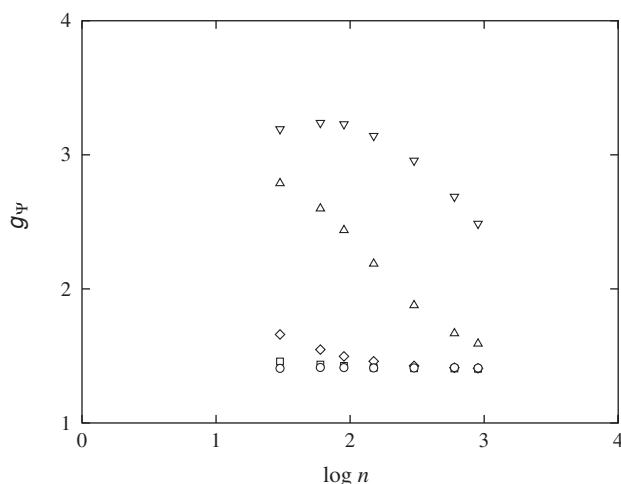


Figure 6. Plots of g_Ψ against $\log n$ at $T^* = 8.0$ (good solvent system). All the symbols have the same meaning as those in Figure 2.

From eqs 16 and 17, g_{A_2} may be written in the form,

$$g_{A_2} = g_S^{3/2} g_\Psi \quad (18)$$

where g_Ψ is the ratio of Ψ_{ap} of the regular three-arm star chain to that of the corresponding linear one. Figure 6 shows plots of g_Ψ against $\log n$ at $T^* = 8.0$ (good solvent system), where all the symbols have the same meaning as those in Figures 2 and 4. It is seen that g_Ψ remarkably increases with increasing θ (chain stiffness). From eq 18 with the results shown in Figures 2, 4, and 6, it may be said that the increase in g_Ψ compensates the decrease in $g_S^{3/2}$ and therefore g_{A_2} is insensitive to change in θ (chain stiffness).

CONCLUSION

We have examined the effects of chain stiffness on the ratio g_{A_2} of A_2 of the regular three-arm star chain to that of the corresponding linear one on the basis of the MC results for A_2 and $\langle S^2 \rangle$ of the freely rotating chains with the LJ 6-12 potential corresponding to a good solvent system. It is found that g_{A_2} is rather insensitive to change in chain stiffness in contrast to the cases of the ratios g_S and g_η related to $\langle S^2 \rangle$ and $[\eta]$, respectively, which remarkably decrease with increasing chain stiffness. Such characteristic behavior of g_{A_2} may be regarded as arising from the fact that in terms of the (classical) perturbation theory,⁴ the effects of the multiple intermolecular contact become negligibly small, if any, in the rigid-rod limit, or in other words, the increase in

the ratio g_Ψ related to Ψ_{ap} compensates the decrease in $g_S^{3/2}$.

Received: July 17, 2008

Accepted: July 29, 2008

Published: September 11, 2008

REFERENCES AND NOTES

1. D. Ida and T. Yoshizaki, *Polym. J.*, **39**, 1373 (2007).
2. D. Ida, Y. Nakamura, and T. Yoshizaki, *Polym. J.*, **40**, 256 (2008).
3. J. G. Kirkwood and J. Riseman, *J. Chem. Phys.*, **16**, 565 (1948).
4. H. Yamakawa, "Modern Theory of Polymer Solutions," Harper & Row, New York, 1971. Its electronic edition is available on-line at the URL: <http://www.molsci.polym.kyoto-u.ac.jp/archives/redbook.pdf>
5. B. H. Zimm and R. W. Kilb, *J. Polym. Sci.*, **37**, 19 (1959).
6. I. M. Irurzun, *J. Polym. Sci., Part B: Polym. Phys.*, **35**, 563 (1997).
7. M. L. Mansfield and W. H. Stockmayer, *Macromolecules*, **13**, 1713 (1980).
8. B. H. Zimm and W. H. Stockmayer, *J. Chem. Phys.*, **17**, 1301 (1949).
9. J. F. Douglas and K. F. Freed, *Macromolecules*, **17**, 1854 (1984).
10. W. G. McMillan and J. E. Mayer, *J. Chem. Phys.*, **13**, 276 (1945).
11. J. P. Hansen and I. R. McDonald, "Theory of Simple Liquids," 3rd ed., Academic, London, 2006.
12. H. Yamakawa and T. Yoshizaki, *J. Chem. Phys.*, **118**, 2911 (2003).
13. H. Yamakawa and T. Yoshizaki, *J. Chem. Phys.*, **119**, 1257 (2003).
14. M. Lal, *Mol. Phys.*, **17**, 57 (1969).
15. N. Madras and A. D. Sokal, *J. Stat. Phys.*, **50**, 109 (1988).
16. N. Metropolis, A. W. Rosenbluth, M. N. Rosenbluth, A. H. Teller, and E. Teller, *J. Chem. Phys.*, **21**, 1087 (1953).
17. S. D. Stellman and P. J. Gans, *Macromolecules*, **5**, 516 (1972).
18. S. D. Stellman, M. Froimowitz, and P. J. Gans, *J. Comput. Phys.*, **7**, 178 (1971).
19. M. Matsumoto and T. Nishimura, *ACM Trans. Model. Comput. Simul.*, **8**, 3 (1998), see also the URL: <http://www.math.keio.ac.jp/matsumoto/emt.html>
20. M. Guenza, M. Mormino, and P. Perico, *Macromolecules*, **24**, 6168 (1991).
21. W. Bruns, *Macromolecules*, **17**, 2826 (1984).
22. H. Yamakawa and T. Yoshizaki, *J. Chem. Phys.*, **121**, 3295 (2004).
23. N. Khasat, R. W. Pennisi, N. Hadjichristidis, and L. J. Fetters, *Macromolecules*, **21**, 1100 (1988).
24. M. Okumoto, Y. Nakamura, T. Norisuye, and A. Teramoto, *Macromolecules*, **31**, 1615 (1998).
25. M. Okumoto, Y. Iwamoto, Y. Nakamura, and T. Norisuye, *Polym. J.*, **32**, 422 (2000).
26. D. Ida and T. Yoshizaki, *J. Chem. Phys.*, in press.
27. P. van der Schoot and T. Odijk, *J. Chem. Phys.*, **97**, 515 (1992).
28. Y. Einaga, F. Abe, and H. Yamakawa, *Macromolecules*, **26**, 6243 (1993).
29. H. Yamakawa, *Macromolecules*, **25**, 1912 (1992).
30. H. Yamakawa, "Helical Wormlike Chains in Polymer Solutions," Springer, Berlin, 1997.
31. K. Ohno, K. Shida, M. Kimura, and Y. Kawazoe, *Macromolecules*, **29**, 2269 (1996).
32. A. J. Barrett, *Macromolecules*, **18**, 196 (1985).